Heteroclinic Cycles in Coupled Systems of Difference Equations

Antonio Palacios
Department of Mathematics
San Diego State University
San Diego, CA 92182-7720
USA

May 31, 2002

Abstract

Cycling behavior, in which solution trajectories linger around steady-states and periodic solutions, is known to be a generic feature of continuous dynamical systems with symmetry. This phenomenon is commonly found in models of coupled cell systems of differential equations. In this type of systems, cycling behavior can even occur as a feature of the global dynamics independently of the internal dynamics of each cell. This conclusion has lead to the discovery of "cycling chaos", in which solution trajectories cycle around symmetrically related chaotic sets. In particular, Dellnitz *et al.* [4] have demonstrated the existence of cycling chaos using Chua's circuit equations and Lorenz equations. In this work, we demonstrate that cycling behavior also occurs in discrete dynamical systems. More specifically, we use the cubic map $f(x, \lambda) = \lambda x - x^3$ to build a coupled system of difference equations, and then prove the existence of structurally stable cycles between fixed points of the dynamics of each cell. Moreover, we use numerical simulations to illustrate that the resulting cycles persist independently of the internal dynamics of each difference equation, as it happens in coupled cell systems of differential equations. Then we demonstrate the existence of cycles involving periodic orbits of the internal dynamics of each cell. Furthermore, we demonstrate that cycling chaos can also occur in coupled systems of difference equations.

1 Introduction

In simple terms, a *heteroclinic cycle* is a collection of solution trajectories that connects sequences of equilibria and/or periodic solutions of continuous and discrete systems. As time evolves, a typical nearby trajectory stays for increasingly longer periods near each solution before it makes a rapid excursion to the next solution. For a more precise description of

heteroclinic cycles and their stability, see Melbourne *et al.* [11], Krupa and Melbourne [9], the monograph by Field [6], and the survey article by Krupa [8]. We should emphasize that although the overall behavior of a heteroclinic cycle is to switch between different forms of solutions or orbits, the switching does not occur periodically. In this sense, heteroclinic cycles and the more common use of the word cycle, which in difference equations is normally associated with periodic orbits, are disntiguished. In what follows, however, we use the word "cycles" to refer to heteroclinic cycles. The existence of structurally stable heteroclinic cycles, i.e., cycles whose topology can not be changed by arbitrarily small perturbations, is considered a highly degenerate feature of both types of systems, continuous and discrete. In other words, typically they do not exist. In continuous systems, where the governing equations normally consist of systems of differential equations, it is well-known that the presence of symmetry can, however, lead to structurally stable, asymptotically stable, cycles [5, 7]. First, symmetry forces certain subspaces of the phase-space to be invariant under the governing equations. Then, cycles are formed through saddle-sink connections between equilibria and/or periodic solutions that lye on the invariant subspaces. As time evolves, a typical nearby trajectory would stay for increasingly longer periods of time lingering around each equilibrium or periodic solution. And since saddle-sink connections are structurally stable so are the cycles.

For systems whose symmetries are described by the continuous group $\mathbf{O}(\mathbf{2})$, i.e. the group of rotations and reflections on the plane, Armbruster *et al.* [1] show that heteroclinic cycles between steady-states can occur stably, and Melbourne *et al.* [11] provide a method for finding cycles that involve steady-states as well as periodic solutions. For systems with discrete symmetries, in particular Dihedral $\mathbf{D}_n$ symmetry, Buono *et al.* [2] show that cycles connecting steady-states and periodic solutions are also found stably in systems of coupled identical cells. Regardless of the type of symmetry in the system, when a heteroclinic cycle is also asymptotically stable, it can serve as a model for a certain kind of intermittency, since nearby trajectories move quickly between solutions (equilibria and periodic solutions) and stay for a relatively long time near each solution.

Similar structures of saddle-sink connections can also lead, in principle, to more complex cycles. The only requirement is for the invariant subspace to contain more complicated type of solutions. For instance, replacing the equilibria in the Guckenheimer-Holmes system with chaotic attractors can lead to what Dellnitz *et al.* [4] call *cycling chaos*. They do this as follows. First, Golubitsky *et al.* [4] show that the Guckenheimer-Holmes system can be interpreted as a network of three identical coupled cells. Using an appropriate choice of coupling function, they model the network by a system of differential equations of the form

$$\frac{dX_i}{dt} = f(X_i) + \sum_{j \to i} \alpha_{ij} h(X_i, X_j), \tag{1}$$

where $X_i = (x_{i1}, \ldots, x_{ik}) \in \mathbf{R}^k$ denotes the state variables of cell i, f governs the internal dynamics of each cell, h is the coupling function between two cells, the summation is taken over those cells j that are coupled to cell i, and α_{ij} is a matrix of coupling strengths. Dellnitz *et al.* [4] then made the critical observation that, under certain conditions, cycling behavior

is a feature of the global dynamics that can persist independently of the internal dynamics of each cell. It follows that if the internal dynamics of the Guckenheimer-Holmes system is replaced by a dynamical system set to produce a chaotic attractor, then the new coupled system would produce cycling chaos. Dellnitz *et al.* demonstrate this conclusion using first Chua's circuit and then Lorenz equations.

Although the existence and stability of heteroclinic cycles in continuous symmetric systems of differential equations has been fully explored, little is known, however, about the existence of these cycles in symmetric systems of difference equations. In previous work [12] we explored numerically the existence of cycling behavior in coupled systems of difference equations. In this work, we now prove the existence of structurally stable heteroclinic cycles between fixed points of a network of coupled cells, where the internal cell dynamics is modeled by one-dimensional iterative maps. We demonstrate that systems of difference equations can also exhibit a wide variety of cycles connecting fixed points with fixed points, and periodic orbits (of arbitrary period) with periodic orbits. More importantly, we show that cycling behavior can also exist independently of the internal dynamics of each cell, as is the case of continuous systems. Consequently, cycling chaos in systems of difference equations is also possible and we illustrate its occurrence with a few examples.

2 Background

2.1 Coupled Cell Systems of Difference Equations

In this work, we consider coupled cell systems similar to those used by Dellnitz *et al.* [4] in the study of cycling chaos, except that now we assume the internal dynamics of each cell to be governed by difference equations. In particular, we consider systems with N identical cells, where the internal dynamics of each cell is governed by a k-dimensional difference equation of the form

$$X_{i_{n+1}} = f(X_{i_n}, \lambda) \tag{2}$$

where $X_i = (x_{i_1}, .., x_{i_k}) \in \mathbf{R}^k$ denotes the state variable of cell i and $\lambda = (\lambda_1, \ldots, \lambda_p)$ is a vector of parameters. A network of cells is a collection of identical interconnected cells, which in the case of N cells it can be modeled by a system of coupled difference equations of the form

$$X_{i_{n+1}} = f(X_{i_n}, \lambda) + \sum_{j \to i} \alpha_{ij} h(X_{i_n}, X_{j_n}), \tag{3}$$

where h is the coupling function between those cells j that are coupled to cell i, $1 \leq i \leq N$, and α_{ij} represents the strength of the coupling. Observe that f is independent of i because the cells are assumed to be identical. Similarly, h is also independent of both i and j due to identical coupling. Additionally, if we let $X = (X_1, \ldots, X_N)$ denote the state variable of the network, then we can write (3) in the simpler form

$$X_{n+1} = F(X_n, \lambda).$$

2.2 Local and Global Symmetries

Following Dellnitz *et al.* [4], we distinguish *local* symmetries from *global* symmetries. $\mathcal{L} \subset \mathbf{O}(k)$ is the group of local or internal symmetries of individual cells if, for all $l \in \mathcal{L}$, we have

$$f(l\,X_i) = l f(X_i).$$

While local symmetries are dictated by f, global symmetries are induced by the pattern of coupling. More precisely, $\mathcal{G} \subset \mathbf{O}(N)$ is the group of global symmetries of the network if, for all $\sigma \in \mathcal{G}$, we have

$$F(\sigma\,X) = \sigma F(X).$$

Depending on the coupling function h, it is possible for the local symmetries l to be also symmetries of the network equations (3). In particular, when the action of l on each cell individually is a symmetry of (3), so that

$$\begin{aligned} h(X_i, l\,X_j) &= l\,h(X_i, X_j) \\ h(l\,X_i, X_j) &= h(X_i, X_j), \end{aligned}$$

for all $l \in \mathcal{L}$, then the coupling is called *wreath product* coupling.

2.3 Case Study: A Network with Three Cells

For illustrative purposes, in the following sections we will consider systems of three identical cells coupled in a directed ring, that is Cell 1 $rightarrow$ Cell 2 $rightarrow$ Cell 3 $rightarrow$ Cell 1. In this case $\mathbf{Z}_3$, the group of cyclic permutations of three objects, is the underlying group of global symmetries of the network. The action of this group is generated by the permutations

$$(x, y, z) \mapsto (z, x, y).$$

Also, we will restrict our analysis to cells whose internal dynamics is one-dimensional, i.e. $k = 1$. We will assume wreath product coupling of identical strength given by $\alpha_{ij} = -\gamma$, where $\gamma > 0$. Next we demonstrate that under these assumptions the corresponding network equations can produce cycling behavior that would connect orbits of the internal dynamics of each cell. Similar ideas can be applied to systems with larger number of cells and with higher dimensional internal dynamics.

3 A Network with Local $\mathbf{Z}_2$ Symmetry

In this Section we consider a network of three cells, where the internal dynamics of an individual cell is governed by the $\mathbf{Z}_2$-symmetric cubic map

$$f(x, \lambda) = \lambda x - x^3, \quad \lambda > 0, \tag{4}$$

where $Z_2 = \{1, -1\}$. The bifurcation diagram of Figure 1 shows that this map exhibits a wide range of complex behavior that includes period-doubling cascades and chaotic attractors. In

fact, the bifurcations in (4) are reminiscent of those found in the *logistic* map [13], except that now local $\mathbf{Z}_2$-symmetry forces two nontrivial fixed points (one with $x > 0$ and one with $x < 0$) to bifurcate from the trivial solution $x = 0$ at $\lambda = 1$. Each fixed point, in turn, undergoes a period-doubling cascade leading to a pair of chaotic attractors. Local $\mathbf{Z}_2$ symmetry again forces the cascades to occur at the same parameter values for each fixed point [3]. For $\lambda < \lambda_c = 3\sqrt{3}/2$, the attractors are confined to opposite sides of the $x = 0$ axis and each attractor has its own basin of attraction. At $\lambda = \lambda_c$, the basins of attraction collide and the two attractors merge into a single one. Rogers and Whitley [14] provide a more comprehensive analysis of a similar map $f(x, a) = ax^3 + (1 - a)x,\ 0 \leq a \leq 4$.

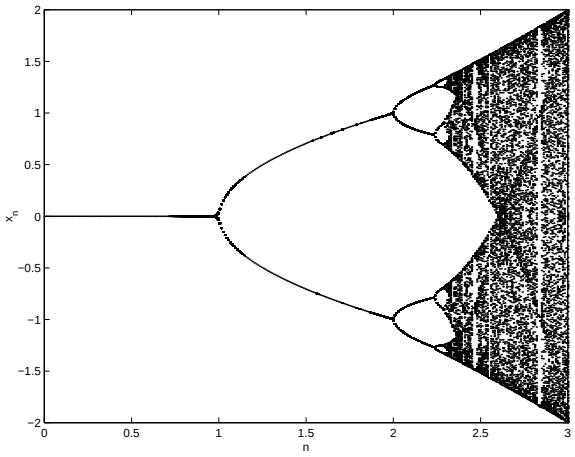

Figure 1: Bifurcation diagram for a cell with internal dynamics $f(x, \lambda) = \lambda x - x^3$.

To form the interconnected network equations (3), we consider a wreath product coupling function of the form

$$h(x_i, x_j) = |x_j|^m x_i, \tag{5}$$

where $0 < m < 1$. Observe that, as expected, h is equivariant under the $\mathbf{Z}_2$ action. The three-cells network, which possesses local $\mathbf{Z}_2$-symmetry and global $\mathbf{Z}_3$-symmetry, then takes the form

$$\begin{aligned} x_n &= \lambda x_n - x_n^3 - \gamma |y|^m x_n \\ y_n &= \lambda y_n - y_n^3 - \gamma |z|^m y_n \\ z_n &= \lambda z_n - z_n^3 - \gamma |x|^m z_n. \end{aligned} \tag{6}$$

The value of the coupling strength γ and the parameter m are critical for the creation of cycling behavior because they control the global dynamics away from the internal dynamics of an individual cell. More specifically, the fact that $0 < m < 1$ prevents the global dynamics from escaping to infinity and controls the rate at which the excursions from the dynamics of one cell to the next one occur. As m decreases, a typical orbit near a cycle spends longer time lingering around the dynamics of an active cell before it makes an excursion to the dynamics of the next cell.

3.1 Existence of Structurally Stable Cycles

To demonstrate the existence of heteroclinic cycles, we assume γ and m to be fixed, and view (6) as a bifurcation problem in λ. We first restrict our attention to the parameter interval $1 < \lambda < 2$, where the internal dynamics of each cell is determined by the nonzero fixed point $\sqrt{\lambda - 1}$. We then seek conditions that can guarantee the existence of structurally stable saddle-sink connections between these fixed points, which are those of the coupled system (6) lying on the orthogonal axes. That is, $E_1(\pm\sqrt{\lambda-1}, 0, 0)$, $E_2(0, \pm\sqrt{\lambda-1}, 0)$, and $E_3(0, 0, \pm\sqrt{\lambda-1})$. Structurally stability will then guarantee that the cycle can persist to small perturbations so long as the symmetry of the network is preserved.

Now, let P_{xy}, P_{xz}, and P_{yz}, denote the orthogonal planes xy, xz, and yx, respectively. Direct calculations of the Jacobian matrix yields the eigenvalues of each fixed point. For each fixed point, the eigenvalues along the tangent directions, i.e. the orthogonal axes, are $\delta_1 = 3-2\lambda$, while on the orthogonal planes the eigenvalues are $\delta_2 = \lambda$ and $\delta_3 = \lambda - \gamma(\lambda-1)^{m/2}$, see Table 1 for a detailed list. The fact that the spectrum of eigenvalues is the same at each fixed point, is a consequence of E_1, E_2, and E_3, being symmetrically related under the action of $\mathbf{Z}_3$, i.e. $\mathbf{Z}_3 \cdot E_1 = E_2$, $\mathbf{Z}_3 \cdot E_2 = E_3$, and $\mathbf{Z}_3 \cdot E_3 = E_1$. These results are needed to assert the existence of a cycle.

Fixed Point	P_{xy}	P_{yz}	P_{xz}
E_1	λ		$\lambda - \gamma(\lambda-1)^{m/2}$
E_2	$\lambda - \gamma(\lambda-1)^{m/2}$	λ	
E_3		$\lambda - \gamma(\lambda-1)^{m/2}$	λ

Table 1: Eigenvalues of fixed points of (6) along the orthogonal x, y and z axes.

Theorem 3.1 *Consider the coupled cell system (6). For $1 < \lambda < 2$, there exists a branch of robust heteroclinic cycles connecting the fixed points (in the same order of appearance) $E_1(\pm\sqrt{\lambda-1}, 0, 0)$ with $E_2(0, \pm\sqrt{\lambda-1}, 0)$ with $E_3(0, 0, \pm\sqrt{\lambda-1})$ if $(\lambda-1)^{m/2} < \gamma < \lambda/f^*$, where $f^* = sup\{\lambda x - x^3\}$ on $1 < \lambda < 2$. The actual sign of the fixed point that the cycle visits depends on the initial conditions of the internal dynamics of each cell.*

Proof: Observe that $\lambda > 0$ implies that the trivial fixed point $(0, 0, 0)$ is subcritically asymptotically stable, while the nontrivial fixed points E_1, E_2, and E_3, are supercritical. In order to prove the existence of a cycle of the form $E_1 \to E_2 \to E_3$, we must show that in each orthogonal plane three conditions are satisfied.

1. Orbits of (6) are invariant.

2. One fixed point is a saddle and the other a sink. Specifically, E_1 is a saddle and E_2 a sink in P_{xy}; E_2 is a saddle and E_3 a sink in P_{yz}; E_3 is a saddle and E_1 a sink in P_{xz}. A cycle in the reverse direction can also be constructed by interchanging saddles and sinks.

3. There are no other fixed points.

4. Orbits are bounded near the origin.

Part 1 follows from direct substitution of $z = 0$, $y = 0$, and $x = 0$ into (6). We verify part 2 as follows. Consider the transition $E_1 \xrightarrow{P_{xy}} E_2$. Since $1 < \lambda < 2$, it follows that $|\delta_1| < 1$, $|\delta_2| > 1$. Also, from the assumption $(\lambda - 1)^{m/2} < \gamma < \lambda/f^*$ and the fact that $f^* = 2\sqrt{8/27} > 1$, we get $(\lambda - 1)^{m/2} < \gamma < \lambda/f^* < \lambda < \lambda/(\lambda - 1)^{m/2}$. Direct work on this last inequality leads to $0 < \lambda - \gamma(\lambda - 1)^{m/2} < 1$, so that $|\delta_3| < 1$. Then it follows from Table 1 that, inside P_{xy}, E_1 is a saddle while E_2 is a sink. $\mathbf{Z}_3$ symmetry forces the spectrum of eigenvalues to be the same on each plane. This fact and the rest of the entries in Table 1 complete part 2. We now verify part 3. On the P_{xy} plane, the only other fixed point is $E_{xy}(\pm\sqrt{x_1}, \pm\sqrt{y_1})$, where $x_1 = \lambda - 1 - \gamma(\lambda - 1)^{m/2}$, and $y_1 = \lambda - 1$. But we just showed that $0 < \lambda - \gamma(\lambda - 1)^{m/2} < 1$, which now implies that $x_1 < 0$ so that no other fixed point exists on P_{xy}. By $\mathbf{Z}_3$ symmetry, this conclusion applies also to the other two planes. We now verify part 4. Consider again the plane P_{xy} and initial conditions within a circle of radius 1. Observe that on the P_{xy} plane the dynamics of the y cell is independent of the x cell. That is, the coupled system has a skew product structure

$$\begin{aligned} x_n &= \lambda x_n - x_n^3 - \gamma |y_n|^m x_n \\ y_n &= \lambda y_n - y_n^3 \end{aligned}$$

Since the y cell behaves freely, we then know (see Figure 1) that if $1 < \lambda < 2$ and $|y_0| < 1$ then $|y_n|$ converges to the fixed point $\sqrt{\lambda - 1}$. We write the dynamics of the x cell in the form $x_{n+1} = (\lambda - \gamma|y_n|^m)x_n - x_n^3$ and interpret y_n as a varying auxiliary parameter so that the principal parameter is now $\lambda_n = \lambda - \gamma|y_n|^m$, i.e. a translation of λ by $\gamma|y_n|^m$. The assumptions $\gamma < \lambda/f^*$ and $1 < \lambda < 2$ imply $0 < \lambda - f^*\gamma < \lambda - \gamma < \lambda_n < \lambda < 2$. Consequently, $0 < \lambda_n < 2$ and if $|x_0| < 1$ then x_n converges to $\sqrt{\lambda_n}$ if $1 < \lambda_n < 2$, or it converges to 0 if $0 < \lambda_n < 1$. But $|y_n| \to \sqrt{\lambda - 1}$ implies that $\lambda_n \to \lambda - \gamma(\lambda - 1)^{m/2}$, and since $0 < \lambda - \gamma(\lambda - 1)^{m/2} < 1$, we then conclude that x_n must converge to 0 and, consequently, (x_n, y_n) remains bounded near the origin. Hence, when $1 < \lambda < 2$, 1-4 show the existence of a structurally stable heteroclinic cycle.

■.

A similar procedure but now applied to F^k can be used to prove the existence of cycles between periodic orbits and chaotic sets. We leave this task for future work. Next, we show results of simulations that include a cycle between fixed points, as is predicted by Theorem 3.1, as well as other type of cycles in which switching between conjugate orbits can occur.

3.2 Results of Simulations

We now verify the existence of a heteroclinic cycle between fixed points, which is guaranteed by Theorem 3.1, through numerical simulations of (6). Additionally, we explore numerically

the implications of the theorem towards the existence of more complicated cycles involving periodic and chaotic orbits. Following the assumptions of Theorem 3.1, we consider first the interval $1 < \lambda < 2$ and coupling strength $\gamma < \lambda/f^*$. Using initial conditions $(x_0, y_0, z_0) = (-0.01, 0.03, 0.02)$ and parameter values $\lambda = 1.5$, $\gamma = 1.0$, $m = 1/2$, simulations of the coupled system (6) reveal the cycle predicted by Theorem 3.1, see Figure 2(a). Observe that when a cell becomes active that cell always selects the same of the two conjugate fixed points of its internal dynamics, either positive or negative. The actual sign of the fixed point that is selected depends on the initial conditions of the active cell.

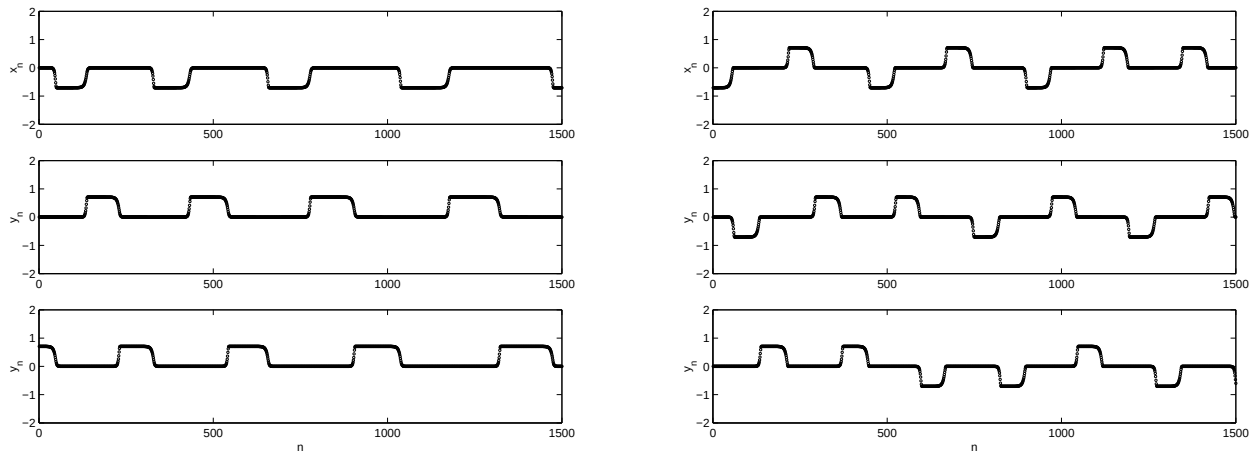

(a) (b)

Figure 2: Two types of cycles connecting fixed points of $f(x, \lambda) = \lambda x - x^3$ at $\lambda = 1.5$. Initial conditions $(x_0, y_0, z_0) = (-0.01, 0.03, 0.02)$. (a) Under weak coupling, $\gamma = 1.0$, an active cell always shows the same of two conjugate solutions. (b) With strong coupling, $\gamma = 2.795$, however, an active cell can switch between two conjugate solutions.

As the coupling strength is gradually increased, a typical orbit near the cycle spends longer time lingering around each fixed point. When γ is increased passed the threshold value λ/f^* the cycle finally disappears. If γ is further increased, however, a second region appears in which cycling behavior is also observed. For instance, Figure 2(b) shows simulation results of a cycle found at $\gamma = 2.75$, all other parameters and initial conditions are the same. Observe that now each cell switches intermittently between conjugate fixed points. In order to get insight into the development of this second type of cycle, we construct two bifurcation diagrams for the coupled cell system (6). In the first diagram, we hold λ fixed while the coupling strength γ varies, and plot the x_n orbit. In particular, we use the same value of λ, i.e. $\lambda = 1.5$, that was used to create the cycles of Figure 2. We also set $x_0 < 0$. The resulting diagram, shown in Figure 3(a), confirms the existence of heteroclinic cycles as predicted by Theorem 3.1. That is, within the region $0.84 \approx (\lambda - 1)^{m/2} < \gamma < \lambda/f^* \approx 1.38$, we observe through the dynamics of the x cell that orbits of the coupled system cycle around

$x = 0$ and the nonzero fixed point $x = -\sqrt{1.5 - 1}$. In every one of these cycles, when the x cell becomes active that cell always selects the same fixed point. For larger values of the coupling strength, such as $\lambda > 2.5$, the diagram reveals the appearance of the second type of cycling behavior that was depicted in Figure 2(b), so that when a cell becomes active, that cell has the ability to switch between conjugate fixed points without changing its initial conditions. To construct the second bifurcation diagram, we hold γ fixed and vary λ. We set $\gamma = 2.75$ so that we can get insight into the cycles that appear when the coupling is strong. The diagram, see Figure 3(b), reveals that for a fixed value of λ, within the approximate interval $1.3 < \lambda < 3$, the activity of the x cell can switch between conjugate orbits of its local dynamics, as is determined by the value of λ in (4).

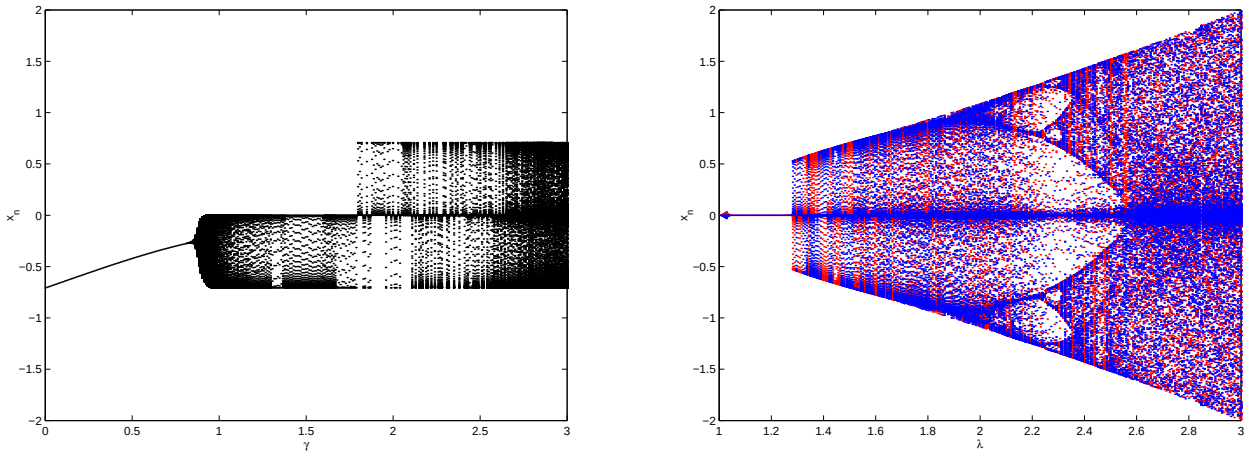

(a) (b)

Figure 3: Bifurcation diagrams of the coupled cell system (6). (a) For weak coupling ($0.84 < \gamma < 1.38$), at $\lambda = 1.5$ the orbit around an active x cell always exhibits the same fixed point. With significantly stronger coupling, however, the orbit can switch between conjugate fixed points. (b) For $1.3 < \lambda < 3$ and $\gamma = 2.795$, the global dynamics makes repeated excursions between zero and the two conjugate orbits of the local dynamics of the x cell.

For λ in $2 < \lambda < \lambda_c$, the internal dynamics of each cell in (6) undergoes a period-doubling cascade leading to a pair of chaotic attractors as was shown in Figure 1. Under a suitable selection of values for the other parameters, we also find trajectories that cycle around the orbits generated by the internal dynamics of each cell. That is, if at a specific value of λ the internal dynamics of each cell produces a periodic orbit, then we expect to find a cycle connecting those periodic orbits. In a similar fashion, we can expect to find cycles that make repeated excursions between chaotic attractors, so long as the main bifurcation parameter is set to yield a chaotic orbit for the internal dynamics of each cell. A typical trajectory in any of these cycles produces a pattern in which, at any given time, one of the cells is active (in a fixed point, periodic orbit or chaotic orbit) while the remaining two are quiescent.

Depending on the coupling strength, two types of cycling patterns are also observed. With relatively weak coupling, an active cell always visits the same of two conjugate orbits, as in Figure 2. With strong coupling, we find again a second type of cycle in which the active cell can switch intermittently between conjugate orbits. For instance, Figure 4 illustrates a cycle of the former type (same conjugate orbit) involving period-two orbits. These orbits are found near the period-doubling bifurcation of the nonzero fixed point, i.e. near $\lambda = 2$. To aid in the visualization of the cycle, continuous lines are superimposed over the discrete orbits. As the period-doubling cascade in the internal dynamics of each cell evolves, cycles involving periodic orbits of higher period also occur robustly. A representative example with random switching between conjugate period-4 orbits is shown in Figure 5.

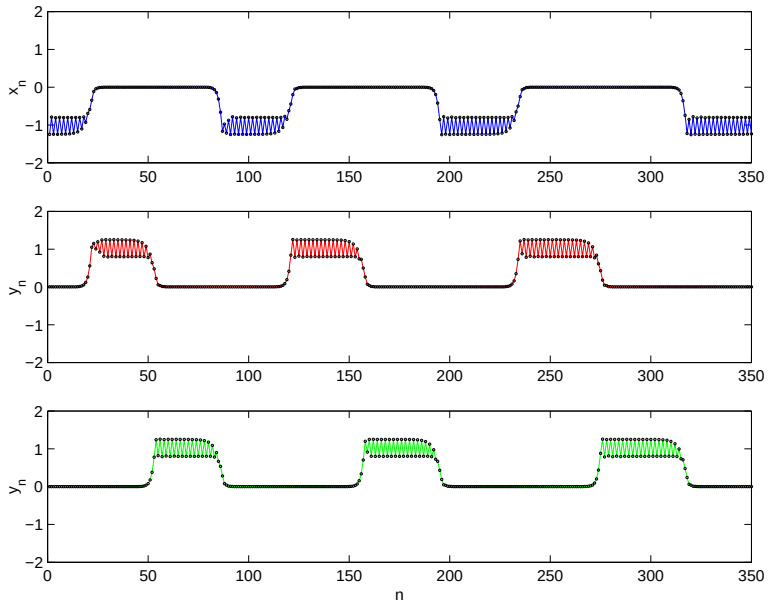

Figure 4: Heteroclinic cycle connecting period-two orbits of $f(x, \lambda) = \lambda x - x^3$. Parameters are: $\lambda = 2.2$, coupling strength $\gamma = 1.7$, and $m = 1/2$. Initial conditions $(x_0, y_0, z_0) = (-0.01, 0.03, 0.02)$.

Cycling behavior also occurs at values of the bifurcation parameter (within $1 \leq \lambda \leq \lambda_c$) where the attractor is a chaotic orbit. For instance, at $\lambda = 2.44$ calculations of Lyapunov exponents (not shown for brevity) confirm the existence of an asymmetric chaotic attractor filling parts of the interval [0,2]. Local $\mathbf{Z}_2$ symmetry in the internal dynamics of each cell forces the existence of a conjugate chaotic attractor within [-2,0]. Depending on the coupling strength, we find two types of cycles connecting chaotic orbits. With $\gamma = 2.7$, for instance, we observe through Figure 6 cycling chaos that is qualitatively similar to the one found by Dellnitz *et al.* [4] using Chua's continuous circuit model. That is, an active cell switches randomly between two conjugate chaotic orbits. With a different value of coupling strength $\gamma = 1.9$, the cycling chaos persists but active cells can no longer switch between conjugate chaotic orbits. This latter type of cycle (not shown for brevity) does not seem to appear in

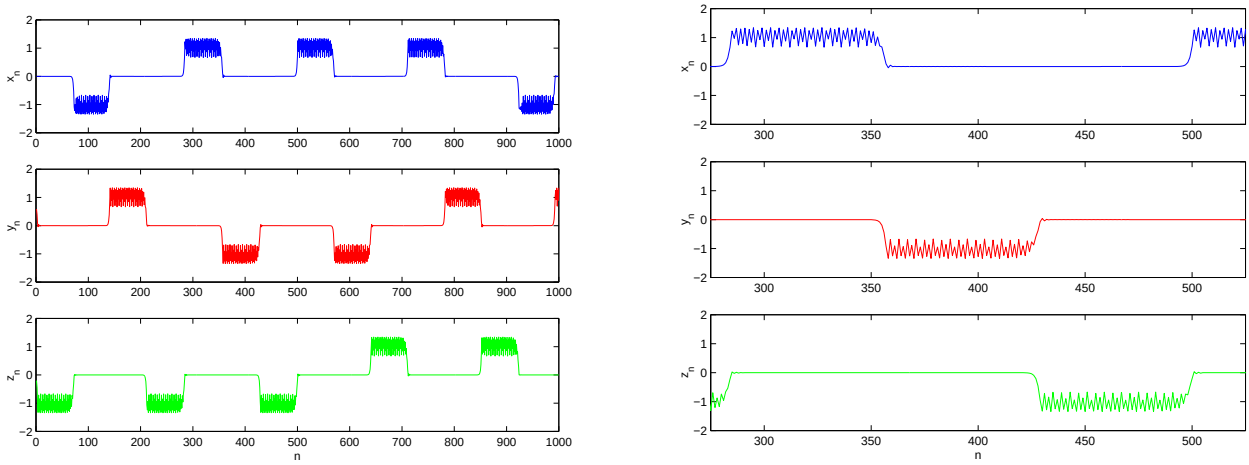

(a) (b)

Figure 5: (a) Heteroclinic cycle connecting period-four orbits of $f(x,\lambda) = \lambda x - x^3$ at $\lambda = 2.3$ and coupling strength $\gamma = 2.91$. Initial conditions $(x_0, y_0, z_0) = (-0.01, 0.03, 0.02)$. Observe that when a cell becomes active that cell can switch between two conjugate period-4 orbits. (b) Magnification of cycle shown in (a).

Dellnitz *et al.* [4].

At $\lambda = \lambda_c$, the basins of attraction of the two chaotic attractors collide and the two attractors merge into one. For values of λ slightly greater than λ_c, Manneville[10] shows that the internal dynamics of each map, in the uncoupled system, produces an intermittent orbit that switches between the remnants of the two attractors. When the cells are coupled, we obtain a third type of cycling chaos (see Figure 7) in which switching between the two remnants of the attractors occurs during the interval of activity of each cell.

4 A Network with Local Trivial Symmetry

In our second example, we assume that the internal dynamics of each cell is governed by the standard logistic map

$$f(x,\lambda) = \lambda x(1-x), \tag{7}$$

where $0 < \lambda < 4$. The local symmetry is now determined by the identity group $\mathbf{1}$. We also employ a wreath product coupling function of the form

$$h(x_i, x_j) = |x_j|^m x_i \tag{8}$$

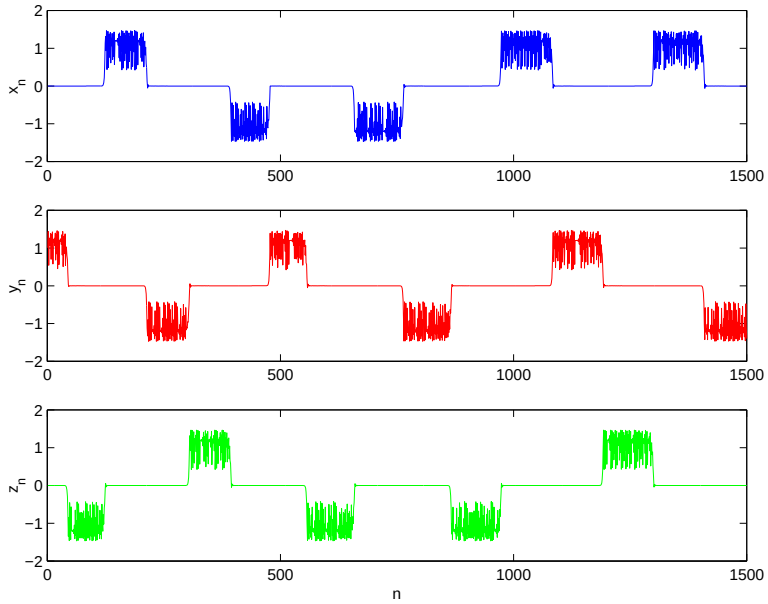

Figure 6: (a) Cycling chaos connecting chaotic attractors of the coupled cell system (6). Parameters are: $\lambda = 2.44$, coupling strength $\gamma = 2.71$, $m = 1/2$. Initial conditions $(x_0, y_0, z_0) = (-0.01, 0.03, 0.02)$.

where $0 < m < 1$. Similar to our previous example, the network equations acquire the form

$$\begin{aligned} x_n &= \lambda x_n(1-x_n) - \gamma|y|^m x_n \\ y_n &= \lambda y_n(1-y_n) - \gamma|z|^m y_n \\ z_n &= \lambda z_n(1-z_n) - \gamma|x|^m z_n. \end{aligned} \tag{9}$$

Different combinations of parameters values for m, λ, and coupling strength γ, yield cycling behavior between orbits of the internal dynamics of each cell. The wide variety of orbits in the logistic map, which now governs the internal dynamics of individual cells, also leads to a full range of cycles connecting fixed points with fixed points, periodic orbits with periodic orbits, and chaotic attractors with chaotic attractors. However, due to the lack of conjugate orbits, there is only one type of cycle in which the same orbit of each cell is always visited by the cycle. For brevity purposes, we illustrate through Figure 8 cycling chaos obtained at two different values of λ where the logistic map is known to yield chaotic orbits. Observe that when $\lambda = 3.8$, cell oscillations are confined to a subinterval of the interval $[0, 1]$, while when $\lambda = 4.0$, the oscillations fill the entire unit interval $[0, 1]$. This behavior is consistent with the chaotic attractors of the logistic map.

5 Conclusions and Future Directions

We have proved that cycling behavior between fixed points of coupled cell systems of difference equations can occur robustly. More importantly, we have shown that, under certain

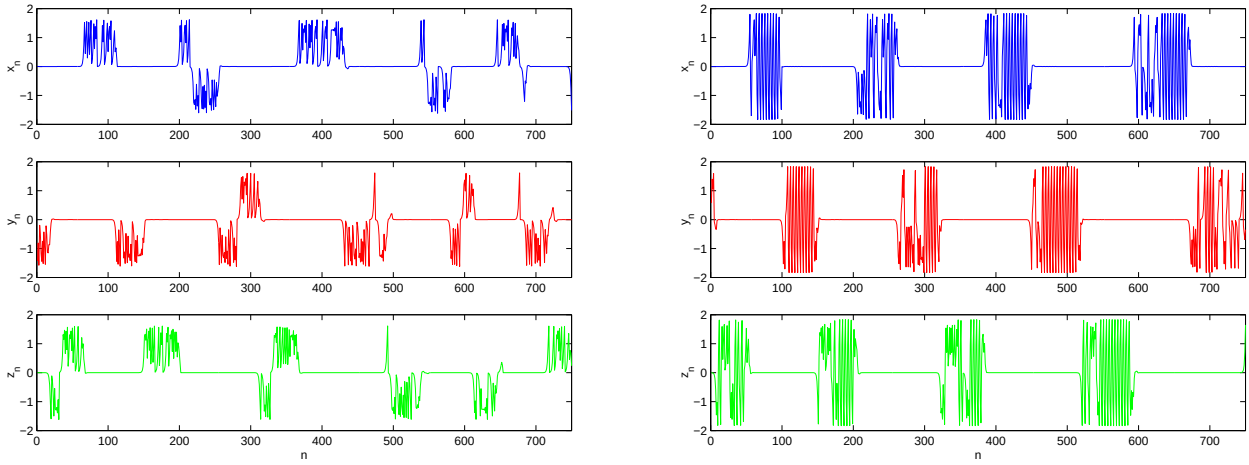

(a) (b)

Figure 7: Intermittent cycling chaos in the coupled cell system (6). Initial conditions $(x_0, y_0, z_0) = (-0.01, 0.03, 0.02)$ (a) Near λ_c, with coupling strength $\gamma = 2.1$, switching between remnants of two chaotic attractors occurs frequently. (b) Away from λ_c, with coupling strength $\gamma = 2.2$, cycling chaos persists and the mergence of the two attractors is more uniform over [0,2].

conditions, when the internal dynamics of individual cells is replaced by periodic orbits, or even chaotic attractors, the cycles persist. Thus, cycling behavior in difference equations, as is the case in their continuous version, can be a global phenomenon that persists independently of the local dynamics of individual cells. Although this assertions has been verified for networks of identical cells, it is still unknown (to the best of my knowledge) whether the cycling phenomenon can persist even if the cells are not exactly identical. To answer this question, the next natural step is to consider networks with near identical cells. Cycling behavior in these latter type of networks, if it exists, could involve excursions between a wider variety of orbits. For instance, we could speculate the existence of a cycle visiting fixed points, periodic orbits, and chaotic attractors, all in one single trajectory of the global dynamics. We anticipate to continue future work in this direction.

Acknowledgments

I would like to thank Prof. Marty Golubitsky for many stimulating conversations.

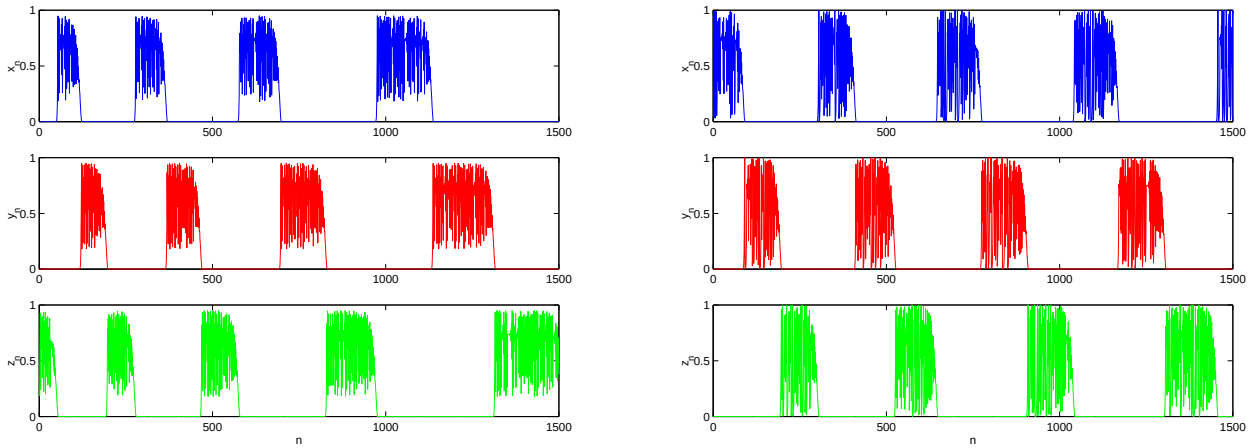

(a) (b)

Figure 8: Cycling chaos in a coupled cell system with internal cell dynamics governed by the logistic map $f(x, \lambda) = \lambda x(1 - x)$. Initial conditions: $(x_0, y_0, z_0) = (0.0161, 0.03, 0.03)$. Parameters are: (a) $m = 10$, $\lambda = 3.8$, and $\gamma = 3.72$, (b) $m = 10$, $\lambda = 4.0$, and $\gamma = 3.97$.

References

[1] Armbruster, D., Guckenheimer, J. & Holmes, P. [1988] "Heteroclinic cycles and modulated traveling waves in systems with $\mathbf{O(2)}$ symmetry," *Physica D* **29**, 257-282.

[2] Buono, P.L., Golubitsky, M. & A. Palacios. [2000] "Heteroclinic cycles in rings of coupled cells," *Physica D* **143**, 74-108.

[3] Dellnitz, M., Field, M., Golubitsky, M., Ma, J. & Hohmann, A. [1995] "Cycling chaos," *Int. J. Bifurc. Chaos* **5**(4), 1243-1247.

[4] Dionne, B. Golubitsky, M., & Stewart, I. [1996] "Coupled cells with internal symmetry. Part I: wreath products," *Nonlinearity* **9**, 559-574.

[5] Field, M.J. [1980] "Equivariant dynamical systems," *Trans. Amer. Math. Soc.* **259**(1), 185-205.

[6] M.J. Field. *Lectures on Bifurcations, Dynamics and Symmetry*. Pitman Res. Notes **356**, Addison-Wesley Longman Ltd., Harlow, 1996.

[7] Guckenheimer, J. & Holmes, P. [1988] "Structurally stable heteroclinic cycles," *Math. Proc. Camb. Phil. Soc.* **103**, 189-192.

[8] M. Krupa. Robust heteroclinic cycles. *J. Nonlin. Sci.* **7** No. 2 (1997) 129–176.

[9] M. Krupa and I. Melbourne. Asymptotic stability of heteroclinic cycles in systems with symmetry. *Ergod. Th. & Dynam. Sys.* **15** (1995) 121–147.

[10] Manneville, P. [1990] *Dissipative Structures and Weak Turbulence.* (Academic Press, Inc.)

[11] Melbourne, I., Chossat, P. & Golubitsky, M. [1989] "Heteroclinic cycles involving periodic solutions in mode interactions with $\mathbf{O}(\mathbf{2})$ symmetry," *Proc. Roy. Soc. of Edinburgh* **113A**, 315-345.

[12] Palacios, A. To appear in [2002] "Cycling chaos in one-dimensional coupled iterated maps," *Int. J. Bifurc. Chaos* **12**(8).

[13] May, R. [1976] "Simple mathematical models with very complicated dynamics," *Nature* **261**, 459-467.

[14] Rogers, T. & Whitley, D.C. [1983] "Chaos in the cubic mapping," *Math. Modelling* **4**, 9-25.